Video Article

Synthesis and Bioconjugation of Thiol-Reactive Reagents for the Creation of Site-Selectively Modified Immunoconjugates

Maria Davydova[1], Guillaume Dewaele Le Roi[1,2], Pierre Adumeau[1], Brian M. Zeglis[1,2,3,4]

[1]Department of Chemistry, Hunter College of the City University of New York

[2]Ph.D. Program in Chemistry, Graduate Center of the City University of New York

[3]Department of Radiology, Memorial Sloan Kettering Cancer Center

[4]Department of Radiology, Weill Cornell Medical College

Correspondence to: Brian M. Zeglis at bz102@hunter.cuny.edu

URL: https://www.jove.com/video/59063
DOI: doi:10.3791/59063

Keywords: Site-specific bioconjugation, site-selective bioconjugation, maleimide, thiol, sulfhydryl, radioimmunoconjugate, immunoconjugate

Date Published: 11/7/2018

Citation: Davydova, M., Dewaele Le Roi, G., Adumeau, P., Zeglis, B.M. Synthesis and Bioconjugation of Thiol-Reactive Reagents for the Creation of Site-Selectively Modified Immunoconjugates. *J. Vis. Exp.* (), e59063, doi:10.3791/59063 (2018).

Abstract

Maleimide-bearing bifunctional probes have been employed for decades for the site-selective modification of thiols in biomolecules, especially antibodies. Yet maleimide-based conjugates display limited stability in vivo because the succinimidyl thioether linkage can undergo a retro-Michael reaction. This, of course, can lead to the release of the radioactive payload or its exchange with thiol-bearing biomolecules in circulation. Both of these processes can produce elevated activity concentrations in healthy organs as well as decreased activity concentrations in target tissues, resulting in reduced imaging contrast and lower therapeutic ratios. In 2018, we reported the creation of a modular, stable, and easily accessible phenyloxadiazolyl methyl sulfone reagent — dubbed 'PODS' — as a platform for thiol-based bioconjugations. We have clearly demonstrated that PODS-based site-selective bioconjugations reproducibly and robustly create homogenous, well-defined, highly immunoreactive, and highly stable radioimmunoconjugates. Furthermore, preclinical experiments in murine models of colorectal cancer have shown that these site-selectively labeled radioimmunoconjugates exhibit far superior in vivo performance compared to radiolabeled antibodies synthesized via maleimide-based conjugations. In this protocol, we will describe the four-step synthesis of PODS, the creation of a bifunctional PODS-bearing variant of the ubiquitous chelator DOTA (PODS-DOTA), and the conjugation of PODS-DOTA to the HER2-targeting antibody trastuzumab.

Introduction

Radiopharmaceutical chemists have long exploited the selectivity and specificity of antibodies for biomarkers of disease for both nuclear imaging and targeted radiotherapy[1]. Far and away the most common approach to the radiolabeling of antibodies is predicated on the indiscriminate attachment of radiolabeled prosthetic groups or radiometal chelators to amino acids — most often lysines — within the structure of the immunoglobulin (**Figure 1A**)[2]. While this strategy is certainly effective, its random, non-site-specific nature can create problems. Specifically, traditional bioconjugation approaches produce poorly-defined and heterogeneous immunoconjugates composed of mixtures of thousands of different regioisomers, each with its own set of biological and pharmacological properties[3]. Furthermore, random bioconjugation can impede the immunoreactivity of antibodies if the cargo is appended to the immunoglobulin's antigen-binding domains.

Over the years, a variety of site-specific and site-selective bioconjugation strategies have been developed in order to address these problems[4,5]. The most common of these approaches relies on the ligation of maleimide-bearing probes to the sulfhydryl groups of cysteines (**Figure 1B**). IgG1 antibodies naturally contain 4 inter-chain disulfide bridges, linkages that can be selectively reduced to yield free thiols capable of undergoing Michael addition reactions with maleimides to form succinimidyl thioether bonds. The use of thiols and maleimides is certainly an improvement over traditional methods, and a wide variety of maleimide-bearing synthons and bifunctional chelators are currently available. However, it is important to note that this methodology has serious limitations as well. Maleimide-based immunoconjugates exhibit limited stability in vivo because the thioether linkage can undergo a retro-Michael reaction (**Figure 2**)[6,7,8,9,10]. This, of course, can lead to the release of the radioactive payload or its exchange with thiol-bearing biomolecules in circulation (e.g., glutathione or serum albumin). Both of these processes can increase activity concentrations in healthy organs as well as decrease activity concentrations in target tissues, resulting in reduced imaging contrast and lower therapeutic ratios. Several alternative thiol-reactive reagents have been developed in an effort to circumvent these issues, including tosylates, bromo- and iodo-acetyls, and vinyl sulfones[11,12,13,14,15,16,17]. However, all of these approaches have limitations that have hampered their widespread application.

About five years ago, the laboratory of the late Carlos Barbas III at Scripps Research Institute pioneered the use of phenyloxadiazolyl methyl sulfones as reagents for the selective formation of highly stable linkages with thiols (**Figure 1C and Figure 3**)[18,19]. The authors employed a phenyloxadiazolyl methyl sulfone-bearing variant of fluorescein to modify several antibodies engineered to contain free cysteine residues, ultimately producing immunoconjugates with higher stability than analogous constructs created using maleimide-based probes. Upon seeing this promising work, we were somewhat surprised that this technology had only been used scarcely in radiochemistry and had not yet been used at all in the synthesis of bifunctional chelators or radioimmunoconjugates[20,21]. This dearth of applications, however, soon began to make more sense: several attempts at procuring the reagent from Sigma-Aldrich resulted in the receipt of complex mixtures of degradation products

with <15% of the desired compound. In addition, synthesizing the reported reagent ourselves was not a realistic option either, as the published synthetic route is somewhat cumbersome and requires sophisticated organic chemistry equipment that most radiochemistry and molecular imaging laboratories — including ours — simply do not possess.

In response to these obstacles, we set out to create an easily accessible and highly stable phenyloxadiazolyl methyl sulfone reagent that can be obtained via a robust and reasonably facile synthetic route. Earlier this year, we reported the creation of a modular, stable, and easily accessible phenyloxadiazolyl methyl sulfone reagent — dubbed 'PODS' — as a platform for thiol-based bioconjugations (**Figure 1C and Figure 3**)[22]. The key difference between PODS and the reagent reported by Barbas, et al. is that the former employs an aniline ring attached to the phenyloxadiazolyl methyl sulfone moiety, while the latter features a phenol in the same position (**Figure 4**). This change facilitates a more straightforward and accessible synthetic route as well as — if our experience with the commercially available compound is emblematic — a more stable final reagent. In this work, we also synthesized a pair of PODS-bearing bifunctional chelators — PODS-DFO and PODS-CHX-A²-DTPA — to facilitate the creation of ^{89}Zr- and ^{177}Lu-labeled radioimmunoconjugates, respectively. As we will discuss, we have demonstrated that PODS-based site-selective bioconjugations reproducibly and robustly create homogenous, well-defined, highly immunoreactive, and highly stable radioimmunoconjugates. Furthermore, preclinical experiments in murine models of colorectal cancer have shown that these site-selectively labeled radioimmunoconjugates exhibit superior in vivo performance compared to radiolabeled antibodies synthesized via maleimide-based conjugations.

The over-arching goal of this work is to facilitate the creation of well-defined, homogeneous, highly stable, and highly immunoreactive immunoconjugates for in vitro and in vivo applications. The synthetic approach is simple enough to be performed in almost any laboratory, and the parent PODS reagent can be modified with a plethora of different chelators, fluorophores, or cargoes. In this protocol and the accompanying video, we will describe the simple, four-step synthesis of PODS (**Figure 5**); the creation of a PODS-bearing variant of DOTA, a widely used chelator for the coordination of ^{64}Cu, ^{68}Ga, ^{111}In, ^{177}Lu, and ^{225}Ac (**Figure 6**); and the bioconjugation of PODS-DOTA to a model antibody, the HER2 targeting IgG1 trastuzumab (**Figure 7**).

Protocol

1. The synthesis of 4-[5-(methylthio)-1,3,4-oxadiazol-2-yl]-aniline (1)

NOTE: Due to the light-sensitivity of the compound, keep all reactions in foil-covered vessels.

1. In a 10 mL round bottom flask, dissolve 100 mg (0.517 mmol, 1 equivalent) of 5-(4-aminophenyl)-1,3,4-oxadiazole-2-thiol in 3 mL of methanol.
2. To this solution, add 360 µL of diisopropylethylamine (DIPEA; 2.07 mmol; 4 equivalents; anhydrous) and a small magnetic stir bar. Cover the flask with a rubber stopper and stir the solution for 10 minutes at room temperature.
3. Using a 1 mL glass syringe, poke a hole through the rubber stopper and quickly add 32 µL (0.517 mmol, 1 equivalent) of iodomethane to this mixture. Allow the mixture to react for 45 minutes at room temperature.
   NOTE: Due to the potential harmful effects of iodomethane, this reaction should be done in a chemical fume hood.
4. Set the water bath of a rotary evaporator to 40 °C and slowly reduce the pressure to remove the solvent to afford a white solid.
5. Dissolve the solid in 3 mL of ethyl acetate and wash at least three times with a 5 mL solution of 0.1 M sodium carbonate using a separatory funnel.
   NOTE: Periodically take spot-tests of the aqueous phase under a UV lamp; once nothing is seen under the lamp, you can stop the washes.
6. Collect the organic phase in a separatory funnel and wash it with water until the pH of the aqueous phase reaches 6.8-7.0 (using pH paper).
7. Collect the organic phase and add magnesium sulfate to remove any traces of water.
   NOTE: The magnesium sulfate should be added with a small spatula, after which the solution should be swirled. If fine particles of the drying agent are still seen, the solution is dry. If not, add small amounts of magnesium sulfate until fine particles can be seen.
8. Filter the mixture using a medium glass frit or filter paper.
9. Evaporate the volatiles using a rotary evaporator, a process which should produce the desired product as white needles.

2. The synthesis of tert-butyl[18-({4-[5-(methylthio)-1,3,4-oxadiazol-2-yl]phenyl}amino)-15,18-dioxo-4,7,10-trioxa-14-azaoctadecyl] carbamate (2)

NOTE: Due to the light-sensitivity of the compound, keep all reactions in foil-covered vessels.

1. In a 25 mL round bottom flask, dissolve 387 mg (0.92 mmol, 1.0 equivalent) of NBoc-N′-succinyl- 4,7,10-trioxa-1,13-tridecanediamine in 10 mL of dichloromethane.
2. To this solution, add 480 µL (2.76 mmol, 3 equivalents) of DIPEA, 264 mg (1.38 mmol; 1.5 equivalents) of N-ethyl-N′-[3-(dimethylamino)propyl]carbodiimide hydrochloride (EDCI), and 200 mg (0.97 mmol, 1.1 equivalents) of **1**. Seal the vessel with a glass stopper and let the reaction stir for 5 days at room temperature.
   NOTE: Be mindful of the evaporation of dichloromethane. If needed, add more throughout the week.
3. Wash the mixture in a separatory funnel with a solution of 1 M hydrochloric acid (3 x 5 mL).
4. Collect the organic phase and continue to wash it in a separatory funnel, first with a solution of 1 M Na_2CO_3 (2 x 5 mL) and then with water (3 x 5 mL).
5. Collect the organic phase and add magnesium sulfate to remove any traces of water (see Step 1.7). Filter the mixture using a medium glass frit or filter paper.
6. Using a rotary evaporator, remove the volatile solvents under reduced pressure to afford an off-white solid.
7. Re-dissolve this solid in 10 mL of ethyl acetate and precipitate the product via the gradual (e.g., 2 mL at a time) addition of 30 mL of cyclohexane.

8. Filter the solution with filter paper or a medium glass frit to obtain the product as a white powder.

3. The synthesis of tert-butyl[18-({4-[5-(methylsulfonyl)-1,3,4-oxadiazol-2-yl]phenyl}amino)-15,18-dioxo-4,7,10-trioxa-14-azaoctadecyl] carbamate (3)

NOTE: Due to the light-sensitivity of the compound, keep all reactions in foil-covered vessels.

1. In a 10 mL round-bottom flask, dissolve 30 mg (0.05 mmol; 1 equivalent) of **2** in 4 mL of dichloromethane.
2. Slowly add in 49 mg (0.2 mmol; 4 equivalents) of 70% m-chloroperbenzoic acid to this mixture and cover the reaction vessel with a glass stopper. Stir the solution overnight at room temperature, ultimately yielding a yellow mixture.
3. Wash the yellow mixture in a separatory funnel, first with a 0.1 M solution of NaOH (3 x 5 mL) and then with water (3 x 5 mL).
4. Dry the organic phase with magnesium sulfate and filter the mixture using a medium glass frit or filter paper.
5. Using a rotary evaporator, remove the solvents under reduced pressure to obtain the product as a pale solid.

4. The synthesis of N^1-(3-{2-[2-(3-aminopropoxy)ethoxy]-ethoxy}propyl)-N^4-{4-[5-(methylsulfonyl)-1,3,4-oxadiazol-2-yl] phenyl} succinamide (PODS)

1. In a 25 mL round bottom flask, dissolve 30 mg of **3** in 2.0 mL of dichloromethane.
2. Add 400 µL of trifluoroacetic acid and seal the flask with a glass stopper.
3. Stir the reaction mixture at room temperature for 3 hours.
4. Using a rotary evaporator, remove the volatiles under reduced pressure at room temperature, leaving an oily residue.
5. Dissolve the oily residue in 7 mL of water and, using a separatory funnel, wash with ethyl acetate (3 x 4 mL). Keep the aqueous layer.
6. Lyophilize the aqueous layer to afford **PODS** as a white powder.
   NOTE: The molar absorption coefficients for PODS at 280 and 298 nm are 9,900 and 12,400 $cm^{-1}M^{-1}$, respectively.

5. The synthesis of PODS-DOTA

1. In a 1.5 mL microcentrifuge tube, dissolve 10 mg of PODS in 300 µL of dimethyl sulfoxide (0.018 mmol; 1 equivalent) and add 26 µL of N,N-diisopropylethylamine (0.15 mmol; 8 equivalents).
2. Dissolve 15.2 mg of DOTA-Bn-NCS (0.02 mmol; 1.2 equivalents) in 100 µL of dimethylsulfoxide and combine this solution with the solution from Step 5.1. Seal the microcentrifuge tube.
3. Allow the reaction to incubate overnight at room temperature.
4. Purify the product using reverse-phase C_{18} HPLC chromatography to remove any unreacted DOTA-Bn-NCS.
   NOTE: Retention times are obviously highly dependent on the HPLC equipment of each laboratory (pumps, columns, tubing, etc.), and appropriate controls should be run prior to purification. However, to present an example, if a gradient of 5:95 MeCN/H_2O (both with 0.1% TFA) to 70:30 MeCN/H_2O (both with 0.1% TFA) over 30 min, a semi-preparative 19 x 250 mm C_{18}column, and a flow rate of 6 mL/min are used, PODS, p-SCN-Bn-DOTA, and PODS-DOTA will have retention times of around 14.4, 18.8, and 19.6 min, respectively. All three compounds can be monitored at 254 nm.

6. The bioconjugation of PODS-DOTA to trastuzumab

NOTE: For this step, we started with a 16.4 mg/mL stock solution of trastuzumab.

1. In a low protein binding 1.5 mL microcentrifuge tube, dilute 61 µL of the trastuzumab stock solution (1 mg; 6.67 nmol, 1 equivalent) with 859 µL of phosphate buffered saline (pH 7.4).
2. To this mixture, add 6.7 µL of a freshly made 10 mM solution of TCEP in H_2O (66.7 nmol, 10 equivalents).
3. Prepare a 1 mg/mL solution of PODS-DOTA in DMSO and add 73 µL of this PODS-DOTA solution to the reaction mixture (66.67 nmol, 10 equivalents).
4. Seal the microcentrifuge tube and incubate the solution for 2 hours at room temperature.
5. After 2 hours, purify the immunoconjugate using a pre-packed disposable size exclusion desalting column.
   1. First, equilibrate the size exclusion column as described by the supplier to remove any preservatives present in the column during storage. A typical procedure involves washing the column 5 times with a volume of PBS that corresponds to the volume of the column: 5 x 2.5 mL of PBS.
   2. Next, add the reaction mixture to the size exclusion column noting the volume of the reaction mixture.
   3. After the reaction mixture has entered the column, add an appropriate amount of PBS to bring the total volume of solution added to the column up to 2.5 mL. For example, if the conjugation reaction resulted in a total volume of 1.3 mL, 1.2 mL of additional PBS would need to be added to the column.
   4. Finally, collect the product using 2 mL of PBS as the eluent.
6. Concentrate the final immunoconjugate with centrifugal filtration units with a 50 kDa molecular weight cut-off.

Representative Results

The first four steps of this protocol — the synthesis — of PODS have been designed to be robust and reliable. The deprotonation and substitution of 5-(4-aminophenyl)-1,3,4-oxadiazole-2-thiol to form the desired thioether product affords the thioether in >99% yield after just 45 minutes. Next, the ligation between **1** and N-Boc-N'-succinyl-4,7,10-trioxa-1,13-tridecanediamine was achieved via a standard peptide coupling procedure, resulting in the collection of the product (**2**) in 55% yield. Then, the oxidation of **2** was performed using m-chloroperoxybenzoic acid, a widely used oxidant. Following the washing steps, **3** was obtained as a pale solid in ~90% yield. Finally, the removal of the tert-butyloxycarbonyl protecting group from **3** was done according to standard procedures, using a 4:1 ratio of dichloromethane:trifluoroacetic acid. After the lyophilization of the aqueous phase, our product — PODS — was obtained as a white powder in 98% yield. The progress of the reaction was followed via thin layer chromatography, and the identity of each product was confirmed via ^{1}H-NMR, ^{13}C-NMR, and HRMS-ESI (**Table 1**).

One of the principal advantages of the PODS reagent is its modularity. A variety of chelators, fluorophores, toxins, or other cargoes can be appended to the compound's pendant amine. In the protocol at hand, we are using the ubiquitous chelator DOTA (1,4,7,10-tetraazacyclododecane-1,4,7,10-tetraacetic acid) as a representative payload. DOTA, of course, has been used in a wide range of biomolecular radiopharmaceuticals as a chelator for radiometals including ^{68}Ga, ^{64}Cu, ^{111}In, ^{90}Y, ^{177}Lu, and ^{225}Ac. To this end, an isothiocyanate-bearing variant of DOTA (p-SCN-Bn-DOTA) was employed and coupled to the pendant amine of PODS via straightforward coupling conditions. The resultant bifunctional chelator was then purified via reverse phase C_{18} HPLC and isolated in ~75% yield. As with the other precursors, the progress of the reaction was followed via thin layer chromatography, and the identity of the product was confirmed via ^{1}H-NMR, ^{13}C-NMR, and HRMS-ESI (**Table 1**).

In the final step of the protocol, we discuss the site-selective bioconjugation of PODS-DOTA to a model immunoglobulin, the HER2-targeting antibody trastuzumab. To this end, the disulfide linkages of the antibody's hinge region are selectively reduced with the reducing agent TCEP [tris(2-carboxyethyl)phosphine]. Following this reduction step, the antibody is incubated with PODS-DOTA for 2 h at room temperature and subsequently purified via size exclusion chromatography. In this case, the purified, DOTA-bearing immunoconjugate was obtained in ~80% yield, and MALDI-ToF analysis revealed a degree of labeling (DOL) of ~1.8 DOTA/mAb. Generally speaking, we have found that 10 equivalents of TCEP, 10 equivalents of the PODS reagent, and a 2 h incubation are sufficient to yield an immunoconjugate with a DOL of 2 PODS/mAb (**Table 2**). This result remains consistent across a range of human, humanized, and chimeric IgG1 antibodies; however, the same conditions produce immunoconjugates with a DOL of only ~1.5 when working with murine IgG1 antibodies. All this said, researchers should optimize these reaction conditions for new antibodies and PODS-bearing cargoes. Finally, and importantly, with respect to the final product, we have repeatedly and reproducibly found that PODS-based immunoconjugates exhibit immunoreactivities equal to or better than analogous constructs created using random or maleimide-based conjugation strategies.

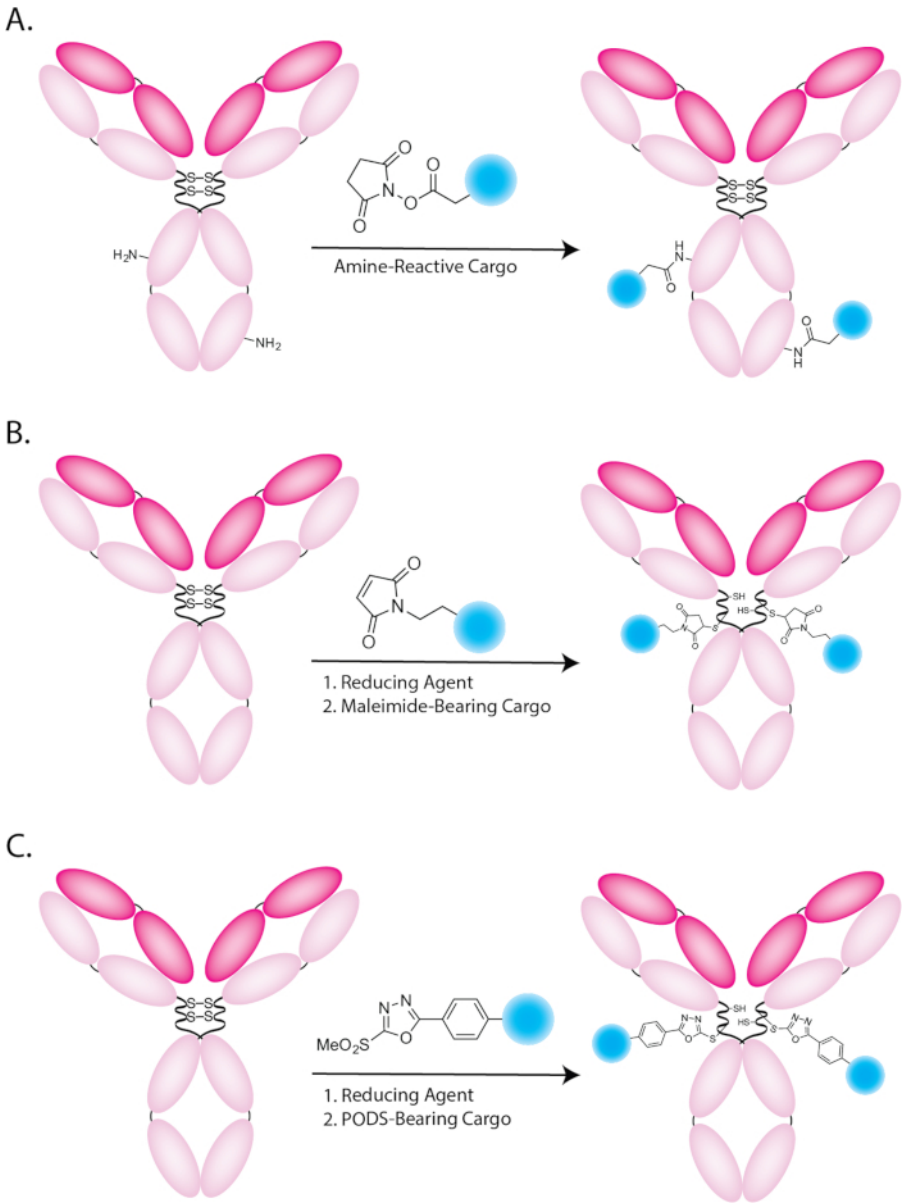

Figure 1: Schematic illustration of bioconjugations using (**A**) amine-reactive, (**B**) maleimide-bearing, and (**C**) PODS-bearing cargoes. Please click here to view a larger version of this figure.

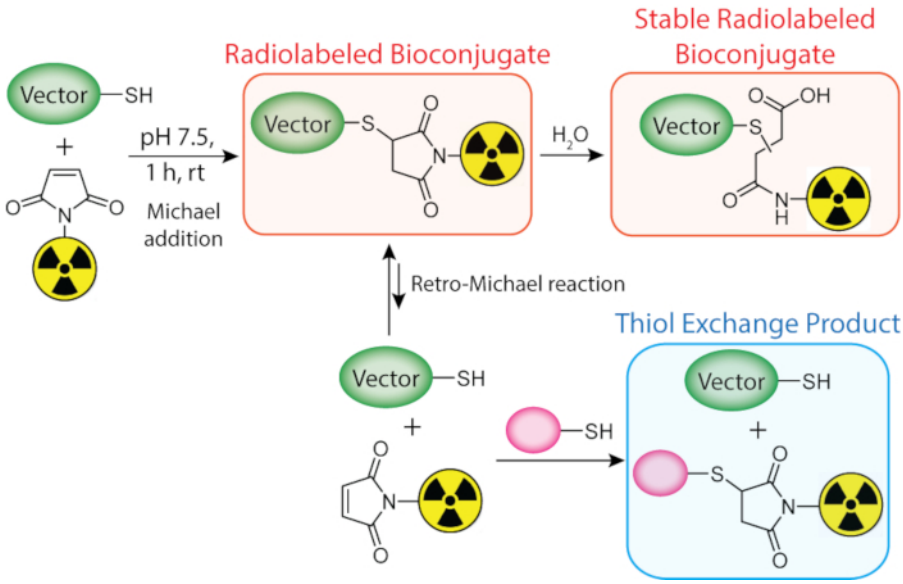

Figure 2: The Michael addition of a thiol-bearing biomolecule (green) and a radionuclide-bearing maleimide (yellow) to form a radiolabeled bioconjugate, as well as the additional reactions that the radiolabeled construct can undergo in the presence of endogenous thiol-bearing molecules (pink). RT = Room temperature. Figure reprinted with permission from Adumeau, P., Davydova, M., Zeglis, B. M. Thiol-Reactive Bifunctional Chelators for the Creation of Site-Selectively Modified Radioimmunoconjugates with Improved Stability. *Bioconjugate Chemistry*. **29**, 1364-1372 (2018). Copyright 2018 American Chemical Society. Please click here to view a larger version of this figure.

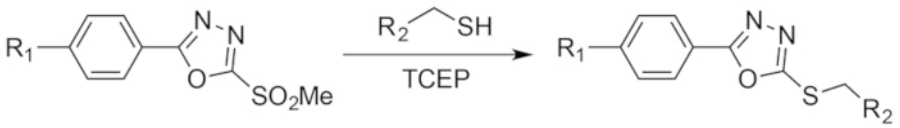

Figure 3: Schematic of the reaction between PODS and a thiol. Figure reprinted with permission from Adumeau, P., Davydova, M., Zeglis, B. M. Thiol-Reactive Bifunctional Chelators for the Creation of Site-Selectively Modified Radioimmunoconjugates with Improved Stability. *Bioconjugate Chemistry*. **29**, 1364-1372 (2018). Copyright 2018 American Chemical Society. Please click here to view a larger version of this figure.

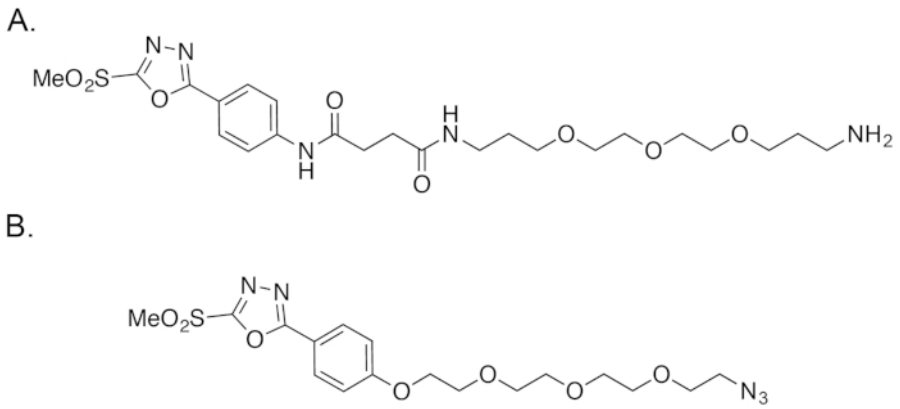

Figure 4: The structure of PODS as well as the reagent reported by Barbas, et al.[18,19] Please click here to view a larger version of this figure.

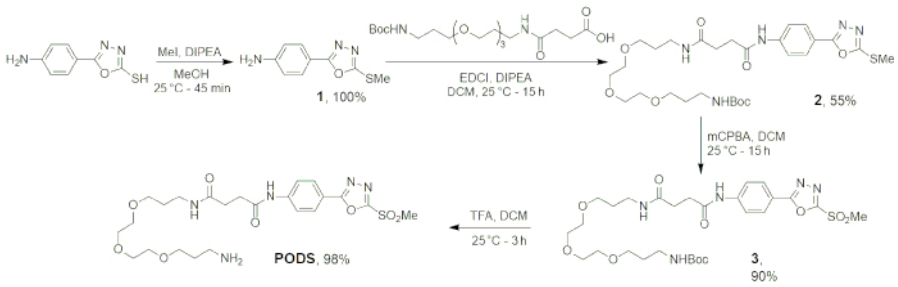

Figure 5: Scheme of the four-step synthesis of PODS. Figure reprinted with permission from Adumeau, P., Davydova, M., Zeglis, B. M. Thiol-Reactive Bifunctional Chelators for the Creation of Site-Selectively Modified Radioimmunoconjugates with Improved Stability. *Bioconjugate Chemistry*. **29**, 1364-1372 (2018). Copyright 2018 American Chemical Society. Please click here to view a larger version of this figure.

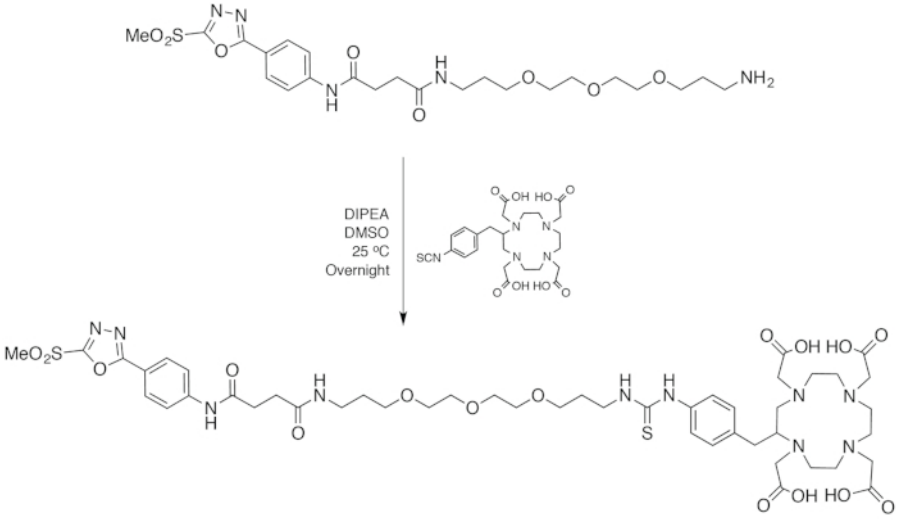

Figure 6: Scheme of the synthesis of PODS-DOTA Please click here to view a larger version of this figure.

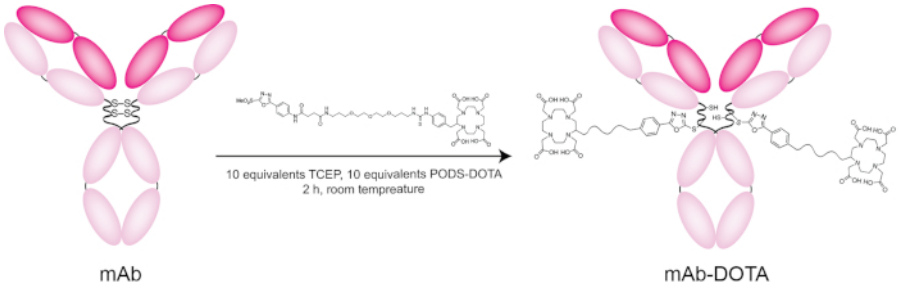

Figure 7: Scheme of the bioconjugation of trastuzumab with PODS-DOTA. Please click here to view a larger version of this figure.

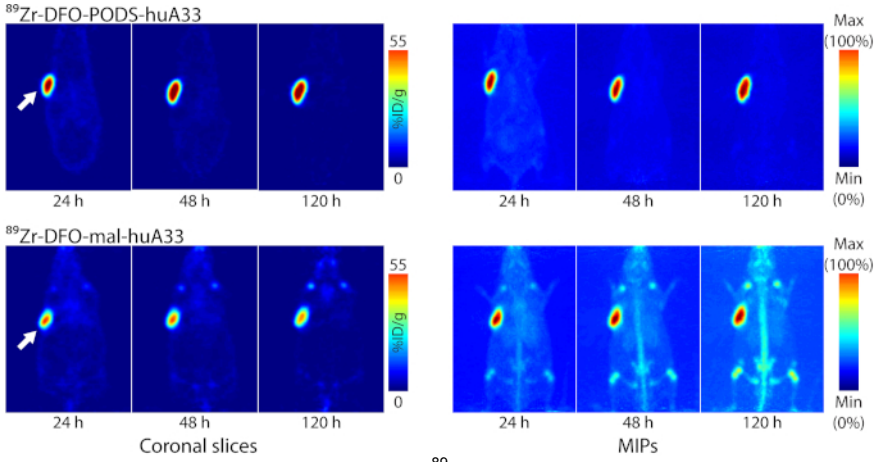

Figure 8: Comparison of the in vivo behavior of ^{89}Zr-labeled radioimmunoconjugates of huA33 created using PODS-based (^{89}Zr-DFO-PODS-huA33) and maleimide-based (^{89}Zr-DFO-mal-huA33) bioconjugation strategies. Planar (left) and maximum intensity projection (right) PET images of athymic nude mice bearing A33 antigen-expressing SW1222 colorectal cancer xenografts (white arrow) following the injection of ^{89}Zr-DFO-PODS-huA33 and ^{89}Zr-DFO-mal-huA33 (140 µCi, 60-65 µg). The coronal slices intersect the center of the tumors. Figure reprinted with permission from Adumeau, P., Davydova, M., Zeglis, B. M. Thiol-Reactive Bifunctional Chelators for the Creation of Site-Selectively Modified Radioimmunoconjugates with Improved Stability. *Bioconjugate Chemistry*. **29**, 1364-1372 (2018). Copyright 2018 American Chemical Society. Please click here to view a larger version of this figure.

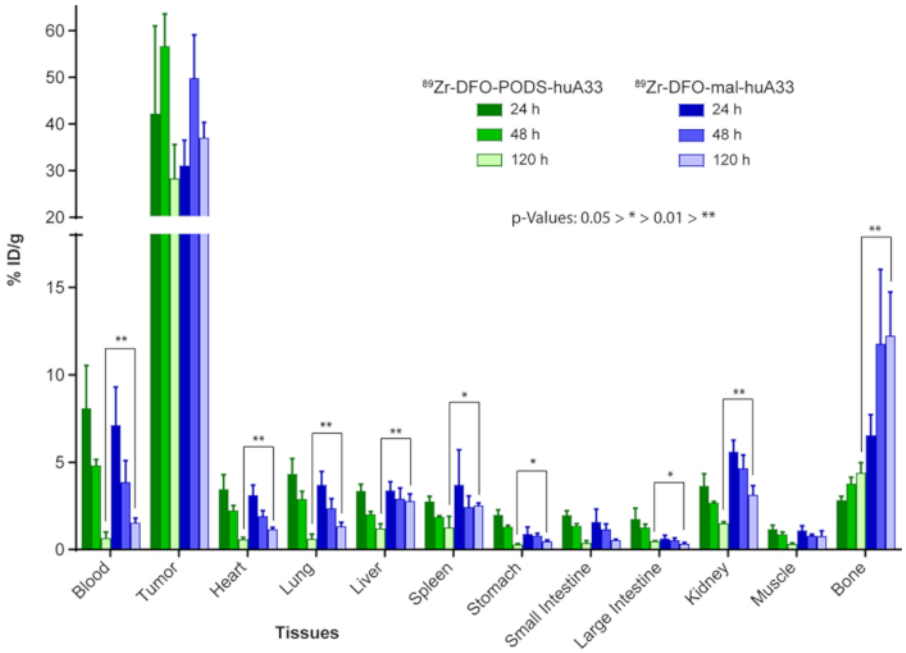

Figure 9: Comparison of the in vivo behavior of ^{89}Zr-labeled radioimmunoconjugates of huA33 created using PODS-based (^{89}Zr-DFO-PODS-huA33) and maleimide-based (^{89}Zr-DFO-mal-huA33) bioconjugation strategies. Biodistribution data after the administration of ^{89}Zr-DFO-PODS-huA33 and ^{89}Zr-DFO-mal-huA33 (30 µCi, 15-18 µg) to athymic nude mice bearing A33 antigen-expressing subcutaneous SW1222 human colorectal cancer xenografts. The values for the stomach, small intestine, and large intestine include contents. Figure reprinted with permission from Adumeau, P., Davydova, M., Zeglis, B. M. Thiol-Reactive Bifunctional Chelators for the Creation of Site-Selectively Modified Radioimmunoconjugates with Improved Stability. *Bioconjugate Chemistry*. **29**, 1364-1372 (2018). Copyright 2018 American Chemical Society. Please click here to view a larger version of this figure.

Compound	^{1}H-NMR Shifts	^{13}C-NMR Shifts	HRMS
1	(500 MHz, $CDCl_3$) 7.79 (2H, d, J = 8.5 Hz), 6.72 (2H, d, J = 8.5 Hz), 4.04 (2H, br s), 2.75 (3H, s)	(125 MHz, $CDCl_3$) 166.3, 163.7, 149.7, 128.5, 114.8, 113.5, 14.8	m/z Calcd for $[C_9H_9N_3OS+H]^+$: 208.0539; found: 208.0539; Δ: 0.0 ppm
2	(500 MHz, CDCl3) 9.68 (1H, s), 7.91 (2H, d, J = 9.0 Hz), 7.71 (2H, d, J = 8.5 Hz), 6.82 (1H, s), 4.99 (1H, s), 3.70-3.45 (12H, m), 3.41 (2H, q, J = 6.0 Hz), 3.20 (2H, q, J = 6.5 Hz), 2.76 (3H, s), 2.71 (2H, m), 2.63 (2H, m), 1.80-1.70 (4H, m), 1.42 (9H, s)	(125 MHz, CDCl3) 172.6, 171.3, 165.8, 164.6, 156.2, 141.8, 127.7, 119.6, 118.6, 79.2, 70.6, 70.5, 70.3, 70.1, 69.6, 38.8, 38.5, 33.5, 31.6, 29.9, 28.6, 14.8	m/z Calcd for $[C_{28}H_{43}N_5O_8S+Na]^+$: 632.2725; found: 632.2722; Δ: -0.47 ppm
3	(500 MHz, $CDCl_3$) 9.99 (1H, s), 7.98 (2H, d, J = 9.0 Hz), 7.75 (2H, d, J = 8.5 Hz), 6.88 (1H, s), 4.99 (1H, s), 3.66-3.50 (15H, m), 3.41 (2H, q, J = 6.0 Hz), 3.20 (2H, q, J = 6.5 Hz), 2.71 (2H, m), 2.65 (2H, m), 1.80-1.70 (4H, m), 1.43 (9H, s)	(125 MHz, $CDCl_3$) 172.6, 171.5, 166.5, 161.6, 156.1, 143.4, 128.7, 119.6, 116.4, 79.1, 70.5, 70.4, 70.2, 70.0, 69.4, 43.0, 38.8, 38.4, 33.2, 31.3, 29.7, 28.4	*m/z* Calcd for $[C_{28}H_{43}N_5O_{10}S+H]^+$: 642.2803; found: 642.2797; Δ: -0.93 ppm
PODS	(500 MHz, D_2O) 7.85 (2H, d, J = 9.0 Hz), 7.55 (2H, d, J = 8.5 Hz), 3.60-3.45 (15H, m), 3.45 (2H, t, J = 6.5 Hz), 3.20 (2H, t, J = 6.5 Hz), 3.04 (2H, t, J = 7.0 Hz), 2.67 (2H, t, J = 6.5 Hz), 2.54 (2H, t, J = 6.5 Hz), 1.87 (2H, qt, J = 6.5 Hz), 1.70 (2H, qt, J = 6.5 Hz)	(125 MHz, D_2O) 174.5, 173.2, 166.8, 161.4, 142.2, 128.6, 120.3, 116.6, 69.4, 69.4, 69.3, 69.2, 68.2, 68.2, 42.5, 37.6, 36.2, 31.9, 30.7, 28.2, 26.4	*m/z* Calcd for $[C_{23}H_{35}N_5O_8S+H]^+$: 542.2279; found: 542.2281; Δ: 0.37 ppm
PODS-DOTA	(600 MHz, DMSO-d_6) 10.46 (1H, s), 9.74 (1H, bs), 8.04 (2H, d, J = 8.6 Hz), 7.99 (1H, s), 7.90 (1H, t, J = 5.0 Hz), 7.86 (2H, d, J = 6.5 Hz), 7.44 (2H, d, J = 7.9 Hz), 7.24 (2H, d, J = 7.1 Hz), 4.35-2.41 (45H, m), 3.70 (3H, s), 1.76 (2H, q, J = 6.3 Hz), 1.61 (2H, q, J = 6.5 Hz)	(125 MHz, DMSO-d_6) 171.8, 171.4, 166.1, 162.2, 158.8, 158.6, 129.8, 129.0, 127.6, 123.3, 119.5, 118.5, 116.5, 116.4, 70.2, 70.1, 70.0, 68.7, 68.5, 43.4, 41.8, 36.3, 32.2, 30.4, 29.8, 29.1	*m/z* Calcd for $[C_{47}H_{68}N_{10}O_{16}S_2+H]^+$: 1093.4334; found: 1093.4327; Δ: -0.64 ppm

Table 1. Characterization data for the synthetic intermediates described as well as PODS and PODS-DOTA.

Antibody	Type	Constant Region	Ratio of PODS:mAb
Human plasma IgG	Human	Human IgG	2.1 ± 0.1
Trastuzumab	Humanized	Human IgG1	2.0 ± 0.1
huA33	Humanized	Human IgG1	2.1 ± 0.1
Cetuximab	Chimeric	Human IgG1	2.2 ± 0.1
AR 9.6	Murine	Murine IgG1	1.4 ± 0.1
Mouse plasma IgG	Murine	Murine IgG	1.5 ± 0.1

Table 2. Degree of labeling of different antibodies following conjugation with a PODS-bearing fluorophore. Values are shown standard deviations. Table reprinted with permission from Adumeau, P., Davydova, M., Zeglis, B. M. Thiol-Reactive Bifunctional Chelators for the Creation of Site-Selectively Modified Radioimmunoconjugates with Improved Stability. *Bioconjugate Chemistry*. **29**, 1364-1372 (2018). Copyright 2018 American Chemical Society.

Discussion

In this report, we have chosen not to include any protocols for radiolabeling or in vivo experimentation. Our reasons are straightforward. With respect to the former, the radiolabeling of a PODS-based immunoconjugate does not differ at all from that of an immunoconjugate synthesized using other bioconjugation strategies, and these procedures have been comprehensively reviewed elsewhere[2]. With regard to the latter, the specifics of preclinical in vivo experiments (i.e., mouse models, doses, etc.) can vary broadly according to both the application and the antibody/antigen system.

Our previous investigations with ^{89}Zr-labeled variants of huA33 provide a compelling illustration of the advantages of PODS-based bioconjugations. HuA33 is a humanized IgG1 antibody that targets the A33 antigen, a transmembrane glycoprotein expressed on >95% of

colorectal cancers[23,24]. In our previous manuscript[22], we report the synthesis of ^{89}Zr-DFO-huA33 radioimmunoconjugate using both PODS- and maleimide-based bioconjugation strategies. The two radiolabeled antibodies — ^{89}Zr-DFO-PODS-huA33 and ^{89}Zr-DFO-mal-huA33 — were produced in nearly identical yield, purity, specificity activity, and immunoreactivity. Critically, however, the two radioimmunoconjugates exhibited dramatically different stabilities in human serum: after incubation for seven days at 37 °C, ^{89}Zr-DFO-PODS-huA33 remained 86 ± 1% intact, while its maleimide-based cousin was only 61 ± 5% intact. In vivo PET imaging and biodistribution experiments in athymic nude mice bearing A33 antigen-expressing SW1222 human colorectal cancer xenografts revealed stark differences in the in vivo behavior of the two radioimmunoconjugates (**Figure 8** and **Figure 9**). Both ^{89}Zr-DFO-PODS-huA33 and ^{89}Zr-DFO-mal-huA33 produce high activity concentrations in tumor tissue: 56.4 ± 6.9%ID/g and 49.6 ± 9.3%ID/g, respectively, 48 h after administration. However, the maleimide-based radioimmunoconjugate produced significantly higher activity concentrations in healthy tissues than the PODS-based agent. For example, ^{89}Zr-DFO-mal-huA33 produced activity concentrations of 3.1 ± 0.5, 2.7 ± 0.4, and 12.2 ± 0.4% ID/g in the kidneys, liver, and bone, respectively, at 120 h post-injection, values which dramatically exceed the activity concentrations produced by ^{89}Zr-DFO-PODS-huA33 in the same tissues (1.4 ± 0.1, 1.2 ± 0.3, and 4.3 ± 0.6% ID/g). Indeed, ^{89}Zr-DFO-PODS-huA33 produced lower activity concentrations in all non-target tissues (except the large intestine) at 120 h post-injection compared to ^{89}Zr-DFO-mal-huA33. As a result, the tumor-to-organ activity concentration ratios for ^{89}Zr-DFO-PODS-huA33 are generally superior to those of ^{89}Zr-DFO-mal-huA33; in particular, the tumor-to-liver, tumor-to-spleen, tumor-to-kidney, and tumor-to-bone activity concentration ratios are nearly double for the PODS-based immunoconjugate compared to its maleimide-derived cousin. Considering that the principal difference between the two radioimmunoconjugates was the bioconjugation handle of the chelator, the increased stability of the PODS-thiol linkage is almost certainly responsible for this improved in vivo performance.

Taking a broader view, the non-site-selective bioconjugation of probes to lysines within antibodies is admittedly a straightforward and facile approach to the modification of antibodies. However, the presence of multiple lysines distributed throughout the structure of immunoglobulins means that it is impossible to exert control over the precise site or degree of bioconjugation[2]. As a result, this random strategy often produces poorly-defined and highly heterogeneous immunoconjugates that can exhibit decreased immunoreactivity if ligations occur within the antigen-binding domains[3]. The benefits of site-selective approaches to bioconjugation have been illustrated repeatedly for both radioimmunoconjugates and antibody-drug conjugates[8,14,25,26,27,28,29,30]. In short, not only do site-selective bioconjugation strategies produce more well-defined and homogenous immunoconjugates than traditional methodologies, they also create imaging agents, radioimmunotherapeutics, and ADCs with improved in vivo performance. Yet where do PODS-based ligations stand in comparison to other site-selective modification strategies? Generally speaking, the approaches to the site-selective modification of antibodies can be classified into four categories: (1) ligations to cysteine residues, (2) the manipulation of the heavy chain glycans, (3) chemoenzymatic transformations, and (4) the use of genetic engineering[4,5]. Of course, this classification system is not perfect, and some approaches (e.g., the modification of the heavy chain glycans with enzymes) inevitably qualify for two categories. Each strategy has its own advantages and disadvantages. Genetic engineering-based approaches provide exquisite control over the site of conjugation, yet they are complex and expensive[31,32,33]. Oxidative couplings to the heavy chain glycans are inexpensive and straightforward, yet they risk oxidative damage to the structural integrity of the immunoglobulin[34,35,36,37,38].

The chief advantage of thiol-based bioconjugations — PODS included — is their simplicity and modularity. Their principal limitation, on the other hand, stems from the presence of multiple thiols within an antibody, a trait which reduces the degree of control over both the site of conjugation and the number of modifications per antibody. In this sense, the combination of thiol-based ligations and antibodies that have been genetically engineered to possess free cysteine residues is a particularly attractive approach. As we have noted, another limitation of maleimide-based thiol ligations is the susceptibility of the succinimidyl thioether bond to retro-Michael additions in vivo. Yet critically, the use of PODS abrogates this problem.

Before we conclude, it is important to note that the emergent nature of PODS technology can create its own set of obstacles. For example, no PODS-bearing bifunctional chelators are (currently) commercially available, and there is no data addressing the clinical pharmacology, toxicology, or immunogenicity of PODS-based immunoconjugates. However, we believe that PODS-based bioconjugations have the potential to fundamentally change the way immunoconjugates are synthesized in both the laboratory and clinic. At present, we have only applied this chemical technology to the development of radioimmunoconjugates for nuclear imaging and radioimmunotherapy, though investigations into the utility of this approach for the construction of antibody-drug conjugates and other biomolecular medicines are currently underway. In the end, we earnestly hope that this protocol — and particularly the straightforward and simple chemistry that we have developed — will help promote the use of phenyloxadiazolyl methyl sulfones for sulfhydryl-based conjugations and spur a shift in the field from maleimides to more stable and more reliable alternatives.

Disclosures

The authors have nothing to disclose.

Acknowledgements

The authors thank Dr. Sai Kiran Sharma for helpful conversations.

References

1. Wu, A. M. Antibodies and antimatter: The resurgence of immuno-PET. *Journal of Nuclear Medicine.* **50** (1), 2-5 (2009).
2. Zeglis, B. M., Lewis, J. S. A practical guide to the construction of radiometallated bioconjugates for positron emission tomography. *Dalton Transactions.* **40** (23), 6168-6195 (2011).
3. Agarwal, P., Bertozzi, C. R. Site-specific antibody-drug conjugates: the nexus of bioorthogonal chemistry, protein engineering, and drug development. *Bioconjugate Chemistry.* **26** (2), 176-192 (2015).
4. Adumeau, P., Sharma, S. K., Brent, C., Zeglis, B. M. Site-specifically labeled immunoconjugates for molecular imaging-part 1: Cysteine residues and glycans. *Molecular Imaging and Biology.* **18** (1), 1-17 (2016).

5. Adumeau, P., Sharma, S. K., Brent, C., Zeglis, B. M. Site-specifically labeled immunoconjugates for molecular imaging-part 2: Peptide tags and unnatural amino acids. *Molecular Imaging and Biology.* **18** (1), 153-165 (2016).
6. Alley, S. C. et al. Contribution of linker stability to the activities of anticancer immunoconjugates. *Bioconjugate Chemistry.* **19** (3), 759-765 (2008).
7. Baldwin, A. D., Kiick, K. L. Tunable degradation of maleimide-thiol adducts in reducing environments. *Bioconjugate Chemistry.* **22** (10), 1946-1953 (2011).
8. Shen, B.-Q. et al. Conjugation site modulates the *in vivo* stability and therapeutic activity of antibody-drug conjugates. *Nature Biotechnology.* **30** (2), 184-189 (2012).
9. Jackson, D. et al. In vitro and *in vivo* evaluation of cysteine and site specific conjugated herceptin antibody-drug conjugates. *Plos One.* **9** (1) (2014).
10. Ponte, J. F. et al. Understanding how the stability of the thiol-maleimide linkage impacts the pharmacokinetics of lysine-linked antibody-maytansinoid conjugates. *Bioconjugate Chemistry.* **27** (7), 1588-1598 (2016).
11. Stimmel, J. B. et al. Site-specific conjugation on serine -> cysteine variant monoclonal antibodies. *Journal of Biological Chemistry.* **275** (39), 30445-30450 (2000).
12. Li, L. et al. Reduction of kidney uptake in radiometal labeled peptide linkers conjugated to recombinant antibody fragments. site-specific conjugation of DOTA-peptides to a cys-diabody. *Bioconjugate Chemistry.* **13** (5), 985-995 (2002).
13. Li, J., Wang, X. H., Wang, X. M., Chen, Z. L. Site-specific conjugation of bifunctional chelator BAT to mouse IgG(1) Fab' fragment. *Acta Pharmacologica Sinica.* **27** (2), 237-241 (2006).
14. Tinianow, J. N. et al. Site-specifically Zr-89-labeled monoclonal antibodies for ImmunoPET. *Nuclear Medicine and Biology.* **37** (3), 289-297 (2010).
15. Li, L. et al. Site-specific conjugation of monodispersed DOTA-PEGn to a thiolated diabody reveals the effect of increasing PEG size on kidney clearance and tumor uptake with improved 64-copper PET imaging. *Bioconjugate Chemistry.* **22** (4), 709-716 (2011).
16. Khalili, H., Godwin, A., Choi, J.-w., Lever, R., Brocchini, S. Comparative binding of disulfide-bridged PEG-Fabs. *Bioconjugate Chemistry.* **23** (11), 2262-2277 (2012).
17. Koniev, O., Wagner, A. Developments and recent advancements in the field of endogenous amino acid selective bond forming reactions for bioconjugation. *Chemical Society Reviews.* **44** (15), 5495-5551 (2015).
18. Patterson, J. T., Asano, S., Li, X., Rader, C., Barbas, C. F., III. Improving the serum stability of site-specific antibody conjugates with sulfone linkers. *Bioconjugate Chemistry.* **25** (8), 1402-1407 (2014).
19. Toda, N., Asano, S., Barbas, C. F., III. Rapid, stable, chemoselective labeling of thiols with Julia-Kocienski-like reagents: A serum-stable alternative to maleimide-based protein conjugation. *Angewandte Chemie-International Edition.* **52** (48), 12592-12596 (2013).
20. Zhang, Q. et al. Last-step enzymatic F-18-fluorination of cysteine-tethered RGD peptides using modified Barbas linkers. *Chemistry-a European Journal.* **22** (31), 10998-11004 (2016).
21. Chiotellis, A. et al. Novel chemoselective F-18-radiolabeling of thiol-containing biomolecules under mild aqueous conditions. *Chemical Communications.* **52** (36), 6083-6086 (2016).
22. Adumeau, P., Davydova, M., Zeglis, B. M. Thiol-reactive bifunctional chelators for the creation of site-selectively modified radioimmunoconjugates with improved stability. *Bioconjugate Chemistry.* **29** 1364-1372 (2018).
23. Sakamoto, J., Kojima, H., Kato, J., Hamashima, H., Suzuki, H. Organ-specific expression of the intestinal epithelium-related antigen A33, a cell surface target for antibody-based imaging and treatment in gastrointestinal cancer. *Cancer Chemotherapy and Pharmacology.* **46** S27-S32 (2000).
24. Sakamoto, J. et al. A phase I radioimmunolocalization trial of humanized monoclonal antibody huA33 in patients with gastric carcinoma. *Cancer Science.* **97** (11), 1248-1254 (2006).
25. Junutula, J. R. et al. Site-specific conjugation of a cytotoxic drug to an antibody improves the therapeutic index. *Nature Biotechnology.* **26** (8), 925-932 (2008).
26. Pillow, T. H. et al. Site-specific trastuzumab maytansinoid antibody-drug conjugates with improved therapeutic activity through linker and antibody engineering. *Journal of Medicinal Chemistry.* **57** (19), 7890-7899 (2014).
27. Boswell, C. A. et al. Enhanced tumor retention of a radiohalogen label for site-specific modification of antibodies. *Journal of Medicinal Chemistry.* **56** (23), 9418-9426 (2013).
28. Boswell, C. A. et al. Impact of drug conjugation on pharmacokinetics and tissue distribution of anti-STEAP1 antibody-drug conjugates in rats. *Bioconjugate Chemistry.* **22** (10), 1994-2004 (2011).
29. Alvarez, V. L. et al. Site-specifically modified In-111 labeled antibodies give low liver backgrounds and improved radioimmunoscintigraphy. *Nuclear Medicine and Biology.* **13** (4), 347-352 (1986).
30. Strop, P. et al. Location matters: SIte of conjugation modulates stability and pharmacokinetics of antibody drug conjugates. *Chemistry, Biology.* **20** (2), 161-167 (2013).
31. Hallam, T. J., Wold, E., Wahl, A., Smider, V. V. Antibody conjugates with unnatural amino acids. *Molecular Pharmaceutics.* **12** (6), 1848-1862 (2015).
32. Axup, J. Y. et al. Synthesis of site-specific antibody-drug conjugates using unnatural amino acids. *Proceedings of the National Academy of Sciences.* **109** (40), 16101-16106 (2012).
33. Lang, K., Chin, J. W. Cellular incorporation of unnatural amino acids and bioorthogonal labeling of proteins. *Chemical Reviews.* **114** (9), 4764-4806 (2014).
34. Yamasaki, R. B., Osuga, D. T., Feeney, R. E. Periodate oxidation of methionine in proteines. *Analytical Biochemistry.* **126** (1), 183-189 (1982).
35. Wang, W. et al. Impact of methionine oxidation in human IgG1 Fc on serum half-life of monoclonal antibodies. *Molecular Immunology.* **48** (6-7), 860-866 (2011).
36. O'Shannessy, D. J., Dobersen, M. J., Quarles, R. H. A novel procedure for labeling immunoglobulins by conjugation to oligosaccharide moieties. *Immunology Letters.* **8** (5), 273-277 (1984).
37. Panowski, S., Bhakta, S., Raab, H., Polakis, P., Junutula, J. R. Site-specific antibody drug conjugates for cancer therapy. *Mabs.* **6** (1), 34-45 (2014).
38. Hu, M. D. et al. Site-specific conjugation of HIV-1 tat peptides to IgG: a potential route to construct radioimmunoconjugates for targeting intracellular and nuclear epitopes in cancer. *European Journal of Nuclear Medicine and Molecular Imaging.* **33** (3), 301-310 (2006).

